



Joint interpretation and modeling of potential field data for mapping groundwater potential zones around Debrecen area, Eastern Hungary

Musaab A. A. Mohammed¹ · Norbert P. Szabó¹ · Péter Szűcs¹

Received: 28 June 2023 / Accepted: 18 December 2023
© The Author(s) 2024

Abstract

The Debrecen area, as part of the Great Hungarian Plain (GHP), is associated with a multi-aquifer system that is overly exploited to fulfill the development plans. This research aims to jointly interpret and model gravity and magnetic data to map the subsurface geology and structures that govern groundwater occurrence. Various potential field techniques, including spectral analysis, anomaly derivatives, analytical signal, and Euler deconvolution were employed to map the distribution and depth of the buried geological structures. The combination of the potential field techniques enabled the construction of a detailed lineament map, providing valuable insights into the distribution of the subsurface structural features. It was indicated that the main structural trend is NW–SE and NE–SW, that coincides with the main structural trends in Hungary. Subsequently, a lineament density map is derived, indicating that the eastern, central, and northwestern parts of the area form the most promising zones for groundwater prospection. The joint inversion of gravity and magnetic data has further enhanced the understanding of subsurface geology. The depth to the basement rock varied between 1.18 and 2.2 km. The highest depth to the basement meets with thick sedimentary sequences bounded by normal faults forming graben and horst structures. Moreover, the distribution of these sediments is investigated using lithological logs indicating the thickness of the main hydrostratigraphic units in the Debrecen area. These units include Nagyalföld Aquifer, Algyő Aquitard, Endrőd Aquitard, and Miocene Badenian Aquifer units, which mainly consist of sand, silt, marl, and gravel. The recent study demonstrated the effectiveness of the joint interpretation in enhancing the knowledge of lithology and geological structures. However, a detailed geophysical survey is recommended to characterize the hydrostratigraphic units in the Debrecen area.

Keywords Pannonian basin · Gravity · Magnetic · Edge detection · Lineaments density · Joint inversion

✉ Musaab A. A. Mohammed
musab20501@gmail.com

¹ Faculty of Earth and Environmental Science and Engineering, University of Miskolc, Egyetemváros, Miskolc 3515, Hungary

1 Introduction

Recently, the demand for groundwater resources has been increasing globally because of population expansion, development, and climate change, so efficient management of groundwater resources has become crucial. The key affronts in managing groundwater resources are acquiring accurate subsurface geology and hydrogeology information. Understanding the lithological variations and geological structure is essential for characterizing the aquifer's boundary conditions and, thus, facilitating sustainable groundwater management strategies (Dilalos et al. 2022; Mohammed et al. 2023a). The aquifer boundary conditions are crucial in groundwater accumulation, flow, and contaminant transport. This information is traditionally obtained with drilling, which is expensive and time-consuming. Geophysical techniques have become powerful tools for studying subsurface geology for groundwater prospecting (Szabó et al. 2015a). These methods provide an efficient way to investigate subsurface geology without extensive drilling. Potential field methods have been widely employed to study subsurface geology, providing valuable insights into the distribution of lithological units and other geological features (Eldosouky et al. 2020; Melouah and Pham 2021).

In Hajdú-Bihar County, situated within the Pannonian basin, the yearly water withdrawal amounts to 3.5 million cubic meters, with Debrecen being recognized as a key location for extracting groundwater and thermal water within the county (Kozak et al. 2010). Additionally, this figure is increasing due to industry, agriculture, and population growth. Ensuring the sustainable functioning of these systems is crucial, taking into account environmental, technical, and economic considerations (Buday et al. 2015). Excessive production can lead to issues such as compaction, subsidence, and intense vertical water flow originating from the groundwater reservoirs in Debrecen (Bendefy 1968). Geophysical techniques aid in comprehending the geological characteristics of the research area and thereby assessing the potential capacity of the groundwater reservoirs (Szabó et al. 2015b; Fejes et al. 2021; Mohammed et al. 2023b). Moreover, the identification of geological formations can assist in recognizing potential pathways for groundwater movement and areas susceptible to excessive production. Among these methods, gravity and magnetic surveys have proven to be highly effective in characterizing the subsurface geology through their ability to detect variations in the rock's petrophysical properties (Nishijima and Naritomi 2017; Njeudjang et al. 2020; Satyakumar et al. 2022; Abdelrady et al. 2023; Mosbahi et al. 2023).

Gravity and magnetic modeling are instrumental in identifying the location and extent of subsurface structures, such as basins, uplifts, and buried faults (Ekinici and Yigitbaş 2015; Abdelrady et al. 2023). However, modeling these potential field methods may result in non-unique and ill-posed solutions due to their intrinsic ambiguity, an underdetermined algebraic formulation, and sensitivity to measurement errors. Prior knowledge is frequently applied to the inversion method to overcome this drawback to obtain workable solutions. Another way is to jointly interpret these potential field data to reduce the uncertainty of the resulting models. Joint modeling aims to gather reliable information for building a subsurface model of the lithology and structure distribution (Zareie and Moghadam 2019), which can be useful for groundwater prospecting (Elawadi et al. 2012).

In this research, a comprehensive study that jointly interpret and model gravity and magnetic data is presented to delineate the subsurface geological structure and lithology that influence the presence and movement of groundwater and, thus, indicate the potential zones for groundwater accumulation in the Debrecen area. The resulting models will serve

as a valuable tool, allowing for a better understanding of the aquifer's boundary conditions and hydrogeological framework.

2 Study area

2.1 Geography, geology, and tectonic setting

The study area is located around Debrecen City, Eastern Hungary, within the Tisza River watershed and covers about 684 km² (Fig. 1). It is part of the Great Hungarian Plain (GHP), which is considered part of the wider Pannonian basin in central Europe. GHP now has a significant disparity in land surface elevation as a result of neotectonic processes, erosion, and considerable deposition (Kiss et al. 2015). These tectonic changes affected Debrecen area and resulted in an elevation range between 99.8 and 122.6 m above sea level (Fig. 1).

Geologically, the GHP comprises different geological formations, including Quaternary, Pannonian, Miocene, and Pre-Neogene. The surface geology of the study area is composed mainly of Quaternary deposits of the Pleistocene age (Gyalog and Síkhegyi 2005). These deposits consist of fluvial sediments, river sediments, and sandy loess (Timár et al. 2005) (Fig. 2). In general, the thickness of the Quaternary deposits in GHP ranges from 80 to 1500 m forming what the so-called Nagyalföld formation (Haas 2012).

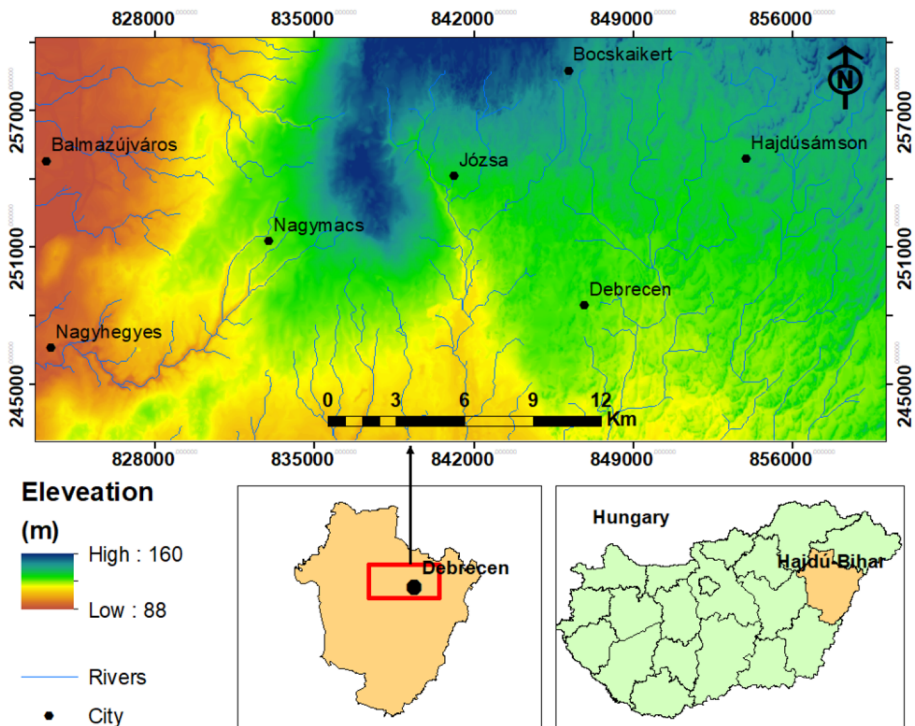


Fig. 1 Geographic map showing the location of the study area

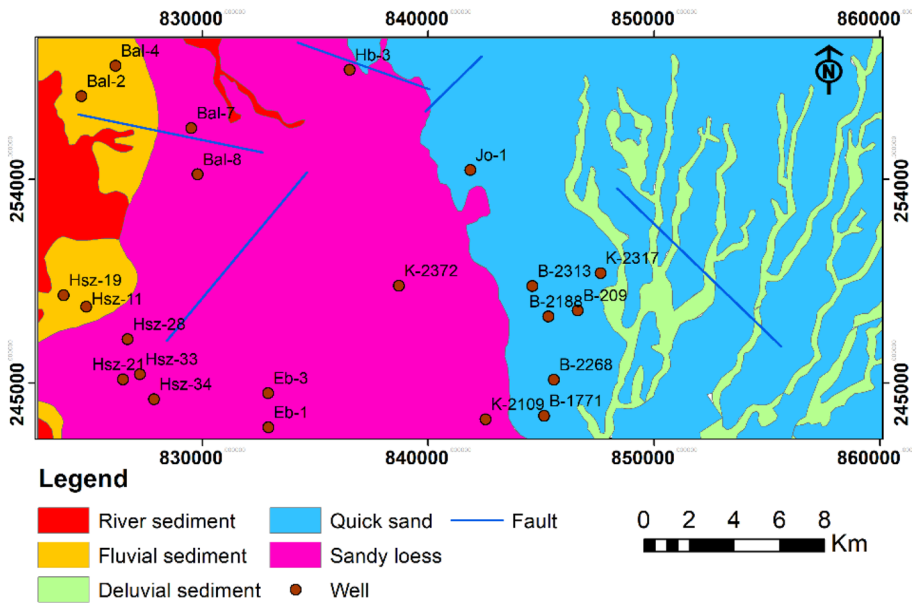


Fig. 2 Geological map showing the main geological units covering the surface of the study area (Gyalog and Sikhegyi 2005)

From a geological perspective, the Pannonian basin is a complicated sedimentary basin composed of several deep localized basins with depths varying from 100 to 7000 m (Tóth and Almási 2001) (Fig. 3). These sedimentary deposits are of Neogene age, i. e., Late Miocene to Pliocene (Horváth 1993), and composed of unconsolidated to semi-consolidated clastic of fluvial, lacustrine, and deltaic. In literature, the Pannonian sediments are divided into two parts, including Lower and Upper Pannonian (Tóth and Almási 2001; Buday et al. 2015). The upper Pannonian is referred to as Pliocene (1.2–5.5 Ma), while the lower Pannonian to the Late Miocene epoch (5.5–11.5 Ma). The Upper Pannonian consists of sequences of sandy delta plain and delta front sediments with alluvial siltstone, sandstone, clay, marl, and quartz pebble beds. These deposits are represented in Újfalu and Zagyva formations (Kronome et al. 2014). In the lower Pannonian, marine incursion submerged the raised island and the lowest part of the high topography, creating a substantial horizontal facies variation. Over only a few kilometers, the coarse-grained sandstone and coastal sandy conglomerates accumulated all over the island are laterally transformed into siltstone (Algyő formation), calcareous marl, and limestone (Endrőd formation). The lower portions of the basin may have delta slopes, depending on the distance of the source area. Sand-silt turbidites with a wide stratigraphic range might accumulate on the distal portions of these slopes (Mádl-Szőnyi and Tóth 2009).

The Badenian Formation is a geological formation that is present in Hungary, particularly in the Transdanubian and North Hungarian basins. It was deposited during the Middle Miocene, around 16.4–13.7 million years ago. The Badenian Formation is composed of various sedimentary rocks such as marl, sandstones, and claystone. The basement rocks of the Hungarian Great Plain are the oldest rocks found in the region, and they form the underlying foundation upon which the overlying sedimentary deposits were laid down. The basement rocks in this area are primarily composed of metamorphic and igneous rocks that

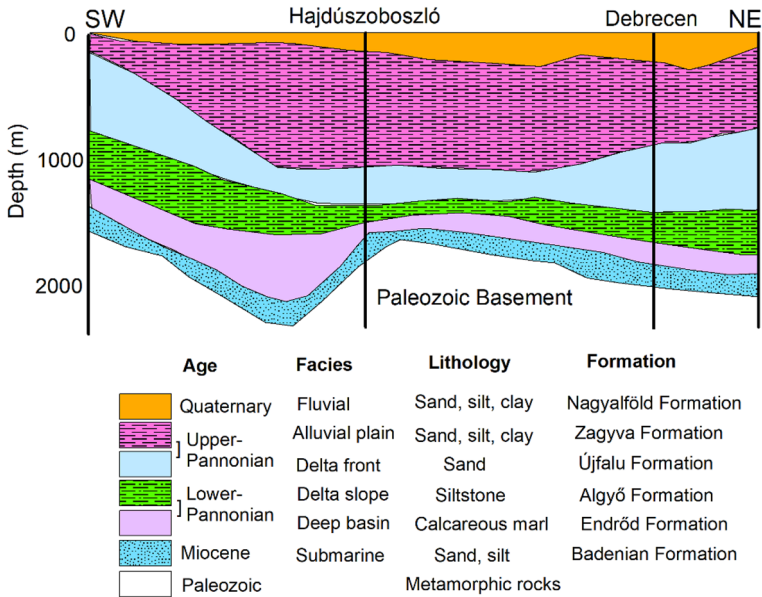


Fig. 3 Geological cross-section modified after Juhász (1991) and (Tóth and Almási 2001), showing the lithology and stratigraphy of the eastern Hungarian Great Plain

were formed during the Paleozoic and Mesozoic eras. The basement rocks in the Hungarian Great Plain are dominated by the Tisza Mega-Unit (Fülöp 1989; Buday et al. 2015). These rocks include granites, gabbros, and basalts, as well as schists and phyllites that were formed through the metamorphism of older sedimentary rocks (Mádl-Szőnyi et al. 2019).

2.2 Hydrostratigraphy and hydrogeology

The main hydrostratigraphic units in the study area include Pre-Neogene aquiclude, Pre-Pannonian aquifer (Badenian), Endrőd aquitard, Algyó aquitard, and the great plain Nagyalföld aquifer (Tóth and Almási 2001). The sedimentary layers covering the basin reached a thickness of more than 5,000 m in the deepest sub-basins. It was discovered that these strata were horizontally extensive and frequently took lenticular forms (Székely et al. 2020).

The Pre-Neogene aquiclude is the bottom hydrostratigraphic unit. This unit is of almost zero permeability that restricts the vertical groundwater flow (Buday et al. 2015). The Pre-Pannonian aquifer is the principal aquifer at the bottom of the groundwater flow basin hosted by the middle Miocene Badenian Formation (Simon et al. 2011). Its high permeability is caused by fracturing and faulting, a large quantity of coarse-grained sediments, and the residual consequences of chemical weathering. The Endrőd and Algyó units are horizontally extensive throughout the study area and composed of calcareous marl and siltstone (Liebe 2006). These units are of low permeability area identified as aquitards (Buday et al. 2015). The Nagyalföld Aquifer, composed of the Quaternary and Újfalu Formations, was identified as the most important shallow aquifer in Hungary (Buday and Püspöki 2011).

Two unique upper and lower hydraulic regimes had developed in the Pannonian Basin. Groundwater flow was predominantly influenced by gravitational forces in the upper regime, whereas overpressure was frequently present in the lower regime (Szűcs et al. 2021). Precipitation served as the main source of recharge in the unconfined gravity-driven zone, whose thickness fluctuated and occasionally exceeded 1,700 m. Debrecen area serves as a transitional zone between the recharge area of Nyírség, which is located in the north-east of the study area and made up of alluvial fans buried with wind-blown sand and the discharge area of Hortobágy, located in the southwest of the study area (Erdélyi 1976). The main factors contributing to the overpressure in the lower regime were the rapid subsidence of marl deposits, basin growth, and basement tectonic processes (Buday et al. 2015). The formation of the overpressure system is impacted by the topography, leading to multiple groundwater flow paths resulting from fractures and sediment windows (Tóth and Almási 2001). Hydraulic interaction between the two regimes commonly happened and was especially important where low-permeability layers pushed outward (Juhász 1991).

3 Materials and methods

This research applied integrated potential field methods to delineate and characterize the subsurface geology for groundwater prospection around Debrecen area, Eastern Hungary. These methods include terrestrial gravity and magnetic. The data used for this study is collected, preprocessed, standardized, and digitized by the Supervisory Authority of Regulating Activities (SZTFH), formerly the Hungarian Mining and Geological Survey (MBFSZ).

3.1 Gravity and magnetic data

In gravity investigation, the geology and the structure of the subsurface are studied using variations in the densities of rocks. The density of rocks close to the surface varies locally, causing slight fluctuations in the gravitational field (Kearey et al. 2002). Gravity data can be employed in numerous hydrogeological and environmental applications, including detecting karsts, tracking aquifer recharge, and mapping the thickness of geological layers and structures (Murty and Raghavan 2002; Darwish et al. 2021). In this study, regional data covering the entire Debrecen is obtained with more than 1900 measurement data, with a density of 4 points per km² (Kiss 2006). During the gravity field survey, the study area is covered with the measurements using gravimeters and acquired relative to a local base network. These base networks were connected to Hungarian and European base stations, including the European Potsdam gravity base level. After performing the necessary corrections of the gravity data, the complete Bouguer anomaly map is calculated in the MGH 50 system (IGSN30, Potsdam basic level) for different correction densities.

In this study, the magnetic data is used to investigate subsurface geology on the basis of variation of magnetic properties of the subsurface. Even though differences in the subsurface water content possess no impact on the earth's magnetic field (Reynolds 2011), magnetic data can be helpful in hydrogeological studies to map out igneous intrusions, identify basin geometry, and locate shallow, local magnetic anomalies that are brought on by geological structures (Rubin and Hubbard 2006). The magnetic data was obtained in the form of the vertical component of magnetic field (ΔZ) that contains 290 data points with a spacing of 1500 m between the stations.

3.1.1 Data correction

The measured gravity values are influenced by several factors, including the elevation of the measurement point, the gravitational attraction of nearby masses, and the centrifugal force due to the earth's rotation. To account for these effects, the gravity data is corrected to remove the estimated influence of these factors. The corrections include terrain correction, free-air correction, and Bouguer correction. Terrain correction is made to account for the gravitational attraction of the topography between the measurement point and a hypothetical reference level (Nowell 1999). Free-air correction is made to account for the reduction in gravitational attraction due to the increase in elevation of the measurement point (Featherstone and Dentith 1997), and Bouguer correction is for the gravitational attraction of the rocks between the measurement point and the reference elevation (Vajk 1956). The corrections were adopted for a density of 2000 kg/m^3 to obtain the complete Bouguer anomaly map (Kiss 2018), and during further processing, these corrected values were used (Fig. 4).

To accurately interpret the magnetic data, corrections are conducted to account for various sources of data noise and distortion. These corrections include diurnal and geomagnetic field corrections. The magnetic data is corrected for diurnal variations due to the daily change in the earth's magnetic field to ensure consistent measurements. Hungarian Magnetic Normal Field value (Kovács and Körmendi 1999) is used to describe the earth's magnetic field at any given time. The magnetic data is corrected to remove the long-wavelength variations in the earth's magnetic field and provide the value of the anomalous magnetic field that is related to the subsurface geology. After performing these corrections, the magnetic anomaly map is obtained for further analysis (Fig. 5). Furthermore, the reduction to pole (RTP) technique is applied to account for the skewness of the resulting anomalies (Baranov and Naudy 1964). The influence of induced magnetization and striking on the configuration of magnetic anomalies is eliminated via RTP, and thus, magnetic anomalies will be relocated to their respective causative bodies. RTP is applied with an inclination of 64.5° and declination of 6.5° . The reduced-to-pole magnetic anomaly map is illustrated in Fig. 6.

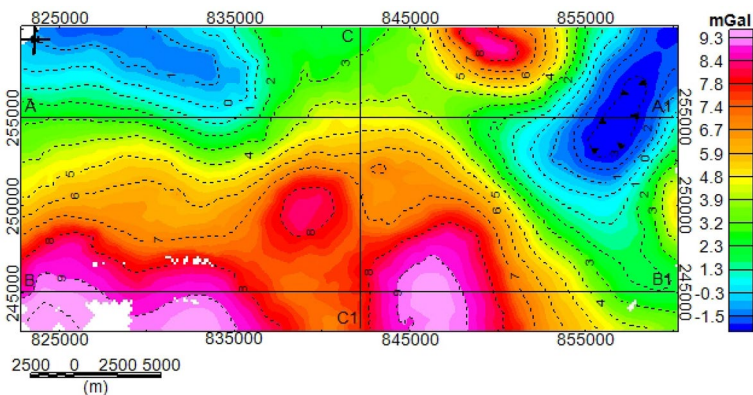


Fig. 4 The complete Bouguer anomaly map of the study area

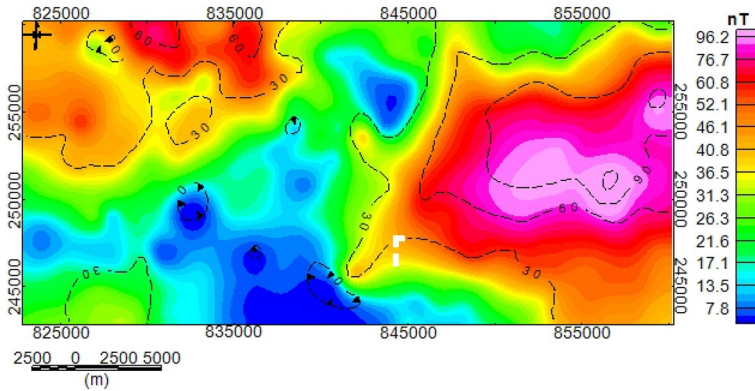


Fig. 5 Vertical component of the magnetic field (ΔZ) referenced to IGRF and corrected for diurnal variation

3.1.2 Data processing

3.1.2.1 Spectral analysis Gravity and magnetic data contain the sum of the effects of different sources, including shallow and deep bodies. These two components are the regional (deep) and residual (shallow) anomalies (Pawlowski 1994). The regional field represents the long-wavelength, low-frequency variations in the potential field data, while the residual anomaly highlights the shorter-wavelength, high-frequency variations. In this study, a Gaussian regional-residual filter with a standard deviation of 0.456 is applied for the anomaly separation. For creating filters to distinguish regional and residual anomaly fields, the power spectrum approach was used (Spector and Grant 1970). Using the Fast Fourier transform (FFT) approach, the spectral analysis is carried out in the wavenumber domain (Sharma and Geldart 1968). FFT shifts the data from the time domain to the frequency domain, aiding in the characterization and modeling of subsurface geology (Blakely 1996).

3.1.2.2 Total horizontal and vertical derivatives The total horizontal derivative (THD) or horizontal gradient of potential field data quantifies the rate of change of the gravitational

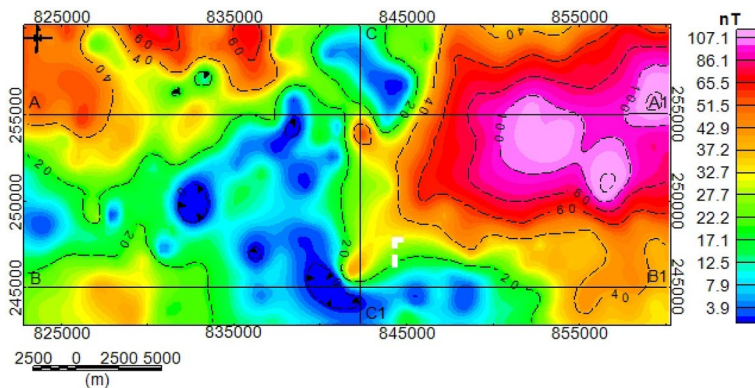


Fig. 6 Reduced to pole delta Z (ΔZ) map

and magnetic fields strength in the horizontal direction (Melouah and Pham 2021). It provides information about the lateral variations in the gravity and magnetic fields with the geological structures located in the highest amplitude of the resulting anomalies (THD > 0) (Mohamed et al. 2022a). The magnitude of the horizontal gradient are calculated as a vector sum of horizontal derivatives of x (E–W) and y (N–S) for the gravity and magnetic data (Núñez-Demarco et al. 2023) (Eq. 1) as

$$THD = \sqrt{\left(\frac{\partial P}{\partial x}\right)^2 + \left(\frac{\partial P}{\partial y}\right)^2} \quad (1)$$

The first vertical derivative (FVD) of gravity and magnetic data captures the rate of change in the gravitational and magnetic fields strength with respect to the vertical direction. It provides insight into the vertical distribution of subsurface density and susceptibility contrasts (Keating 1995). In the analysis of the FVD map, the areas of higher than zero anomalies represent the edge of the causative bodies. It can be obtained by Eq. 2 as

$$FVD = \left(\frac{\partial P}{\partial z}\right) \quad (2)$$

where P represents the gravity and magnetic fields.

3.1.2.3 Tilt angle derivative (TAD) The tilt angle derivative (TAD) is a mathematical transformation used to analyze and interpret gravity and magnetic data. It provides information about the gradient or slope of the fields and is expressed as the ratio of the vertical to the horizontal derivative of the anomalies (Miller and Singh 1994) (Eq. 3).

$$TAD = \tan^{-1} \left[\frac{\frac{\partial P}{\partial z}}{\sqrt{\left(\frac{\partial P}{\partial x}\right)^2 + \left(\frac{\partial P}{\partial y}\right)^2}} \right] \quad (3)$$

TAD is useful in geological mapping, exploration, and understanding the subsurface geological structure. The threshold angle defines the maximum change in the gravity and magnetic anomalies associated with lineament. In this research, a threshold of zero angles is used to identify potential areas for geological features (Verduzco et al. 2004).

3.1.2.4 Analytical signal (AS) The analytical signal (AS) is a complex number that consists of two components, including amplitude and phase (Alvandi et al. 2022). The amplitude of the AS indicates the magnitude of the fields, while the phase provides insights into their orientation (Eldosouky et al. 2020). The 3D AS is calculated as a vector sum of x, y, and z derivatives as (Eq. 4):

$$AS = \sqrt{\left(\frac{\partial P}{\partial x}\right)^2 + \left(\frac{\partial P}{\partial y}\right)^2 + \left(\frac{\partial P}{\partial z}\right)^2} \quad (4)$$

The AS of gravity and magnetic fields helps enhance the interpretation by highlighting the boundaries of the anomalous bodies and providing information about their spatial characteristics (Essa et al. 2021).

3.1.2.5 Lineament extraction and lineament density map The lineaments are identified and traced using different potential field techniques, including field derivatives and analytical signals. The extracted lineaments based on gravity and magnetic data using different techniques are filtered, and a universal lineament map is obtained. The lineament density ($L_{d_{ij}}$) map, as a useful tool for groundwater exploration, is further constructed to identify areas with a high density, which indicates the presence of geological structures that are favorable for groundwater accumulation and flow. The study area is discretized into grid cells, with each grid covering 500 m², and the lineaments density is calculated as the sum of the length of the lineaments within the cell divided by the area of the cell (Eq. 5)

$$L_{d_{ij}} = \frac{\sum_{j=1}^n L_{ij}}{A_i} \quad (5)$$

where L_{ij} denotes the length of the j th lineaments within the i th cell, n is the number of the lineaments, and A_i is the area of the i th cell. The lineament length in each grid is then interpolated to reveal the spatial distribution of the lineament density.

3.1.2.6 3D Euler deconvolution The 3D Euler deconvolution (ED) is designed to estimate the location and depth of the buried geological structures from potential field data (Ghosh 2022; Kenyo et al. 2023). ED technique assumes that the anomalies observed in the gravity or magnetic fields are caused by simple isolated sources, and it searches for the optimal location and depth of these sources by deconvolving the data with a theoretical response function (Thompson 1982). A 3D grid is created to cover the study area, and each grid point represents a potential source location. The ED is performed at each point employing windows and shapes depending on the expected size and shape of the geological structure. This involves finding the optimal combination of coordinates and depth that produces the best fit between the observed and the theoretical response function. The ED can be calculated (Eq. 6) as

$$(x - x_0) \frac{\partial U}{\partial x} + (y - y_0) \frac{\partial U}{\partial y} + (z - z_0) \frac{\partial U}{\partial z} = -NU \quad (6)$$

where U is the total gravity and magnetic field anomalies recorded at the x , y , and z axis, and x_0 , y_0 , and z_0 are the locations of the depth sources. N is the structural index (SI). The range of SI is from 0 to 2, and the variation is based on the depth, type, and orientation of the anomaly sources (Chen et al. 2022). In the current investigation, $SI=0$ as an index used to delineate the vertical and, to some extent, subsurface geological structures has been used and applied to the potential field data.

3.1.2.7 2D joint interpretation and modeling The 2D joint interpretation of gravity and magnetic data is carried out to determine the distribution of the geological structures and the relief of the basement rocks in the study area. The gravity and magnetic data are jointly and interactively inverted using GM-SYS program of Geosoft. This program is based on Talwani et al. (1959) method and (Won and Bevis 1987) algorithm. In forward modeling, a hypothetical two-layered geological model that is assigned to sediments and basement rocks is created, and the geophysical responses to that model are determined. The subsurface layers are represented as polygonal bodies that are constructed using a series of connected vertices. Because of geological heterogeneity, the main polygons that represent the two main layers and the sub-polygons within each layer have associated properties of density

and magnetic susceptibility, which allow mapping the vertical and horizontal heterogeneity. The gravitational potential is typically computed using the 3D Poisson's equation, while the magnetic field is computed using the 3D magnetic field equation (Talwani 1964). The inversion is achieved by interactively minimizing the misfit between the observed and calculated data using the least square method (Webring 1985). The minimization of the objective function is carried out using Marquardt (1963) algorithm. This technique iteratively updates the model parameters to minimize the misfit and converge toward the best-fit solution. In this research, additional constraints are included to stabilize the inversion and prevent oscillatory solutions. These constraints are based on the prior information about the subsurface geology obtained from borehole data and previous geological reports.

4 Results and discussion

Gravity and magnetic data are used in this study to delineate the structural characteristics and the subsurface lithological features that may influence groundwater accumulation in the study area. This is achieved by combining different qualitative and quantitative techniques. The qualitative methods include spectral and gradient analysis, while for quantitative methods, ED and joint model-based inversion techniques for gravity and magnetic data are applied.

4.1 Qualitative interpretation

The Bouguer and magnetic anomaly maps were subjected to radial averaged spectral analysis to guide the residualization and regionalization of the anomaly (Spector and Grant 1970; Basantaray and Mandal 2022). Results of the Bouguer and magnetic spectral analysis are shown in Fig. 7a and b, respectively. The spectra of gravity and magnetic anomaly show three attitudes. The deep and shallow anomaly responses are colored blue and orange, respectively, while the third part of the curve is colored green and attributed to the effect of the data noise. The energy curve's logarithmic decay exhibits a sharp decline for deep sources and a softer decline at shallow sources (Basantaray and Mandal 2022). The noise in the spectral analysis of potential field data appears as a low-amplitude curve that

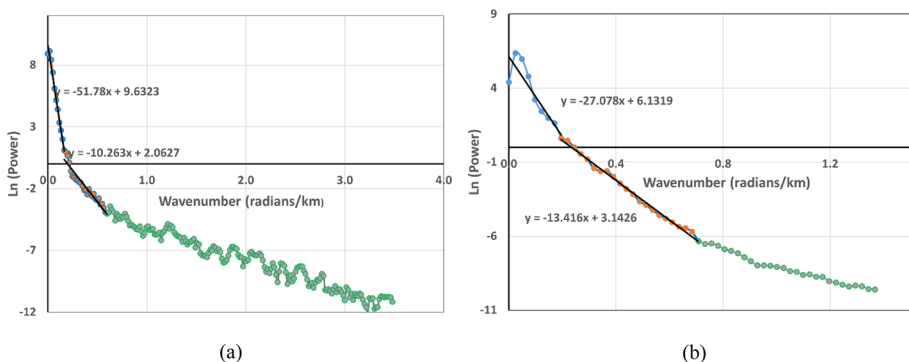


Fig. 7 Spectral analysis of the **a** gravity and **b** magnetic data of the study area. The blue and orange color describes the deep and shallow sources responses, while the green represents the data noise response

extends across a range of frequencies with no distinct peaks (Mohamed et al. 2022b). The shallow zone is described as sedimentary rocks, and the deeper represents a basement rock zone of relatively greater density and susceptibility.

The spectral analysis also resulted in regional and residual maps of Bouguer and magnetic anomaly (Fig. 8) showing deep and shallow features. The Bouguer regional map (Fig. 8a) indicated a high gravity dense body in the southern and southwestern part of the area and local basins with a low anomaly in the northeastern and northwestern part of the area. The magnetic regional anomaly map (Fig. 8b) in return, indicated anomalous bodies in the eastern and northwestern parts of the study area. The major gravity and magnetic anomalies represent significant geological boundaries, including faults resulting in major lithological changes. As a result, regional faults in NW–SE and NE–SW directions are indicated. These are the main trends of the geological structures in eastern Hungary (Bodoky and Balla 2015). These obtained regional lineaments are also supported and verified by geological maps of the study area. The residual anomaly map of Bouguer (Fig. 8c) and magnetic (Fig. 8d) identified the shallow smaller-scale features and potential lineaments for groundwater accumulations. The residual maps of gravity and magnetic anomalies indicated the shallow anomalous bodies throughout the study area with dominant NW–SE and NE–SW lineaments.

The total horizontal derivative (THD) of gravity and magnetic anomaly maps provided information about lateral density and magnetic susceptibility variations associated with geological structures. The THD map of the Bouguer anomaly (Fig. 9a) is associated with distributed anomaly throughout the study area, with the lineaments in the highest amplitude trending mostly in NW–SE and NE–SW directions. THD map indicated negative anomalies due to the kriging interpolation method used to map the values. The THD map of the magnetic anomaly (Fig. 9b) showed major lineaments trending in the NW–SE direction.

The first vertical derivative (FVD) of the gravity field is particularly useful for detecting and characterizing subsurface density variations. Maximum vertical gradients indicate

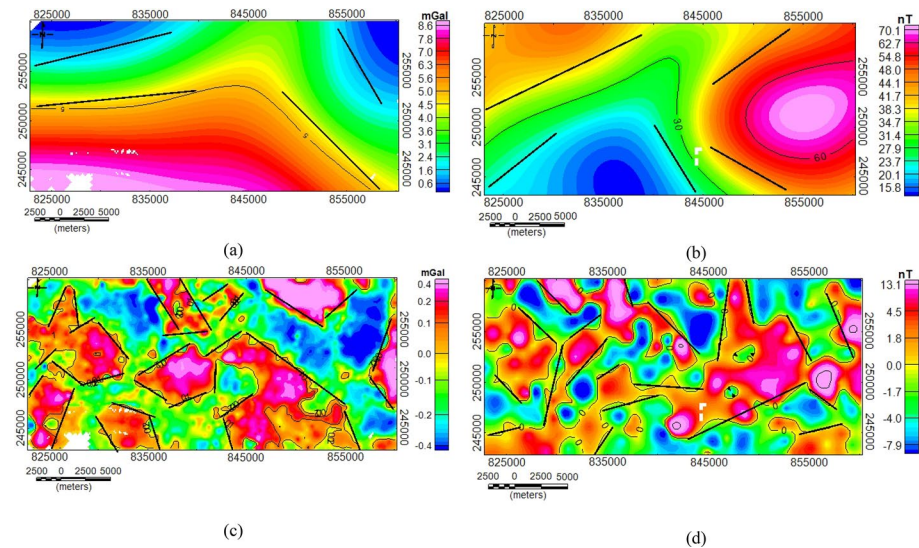


Fig. 8 Regional anomaly of **a** gravity and **b** magnetic data and residual anomaly of **c** gravity and **d** magnetic anomaly data. The geological structures are included and indicated by thick black lines

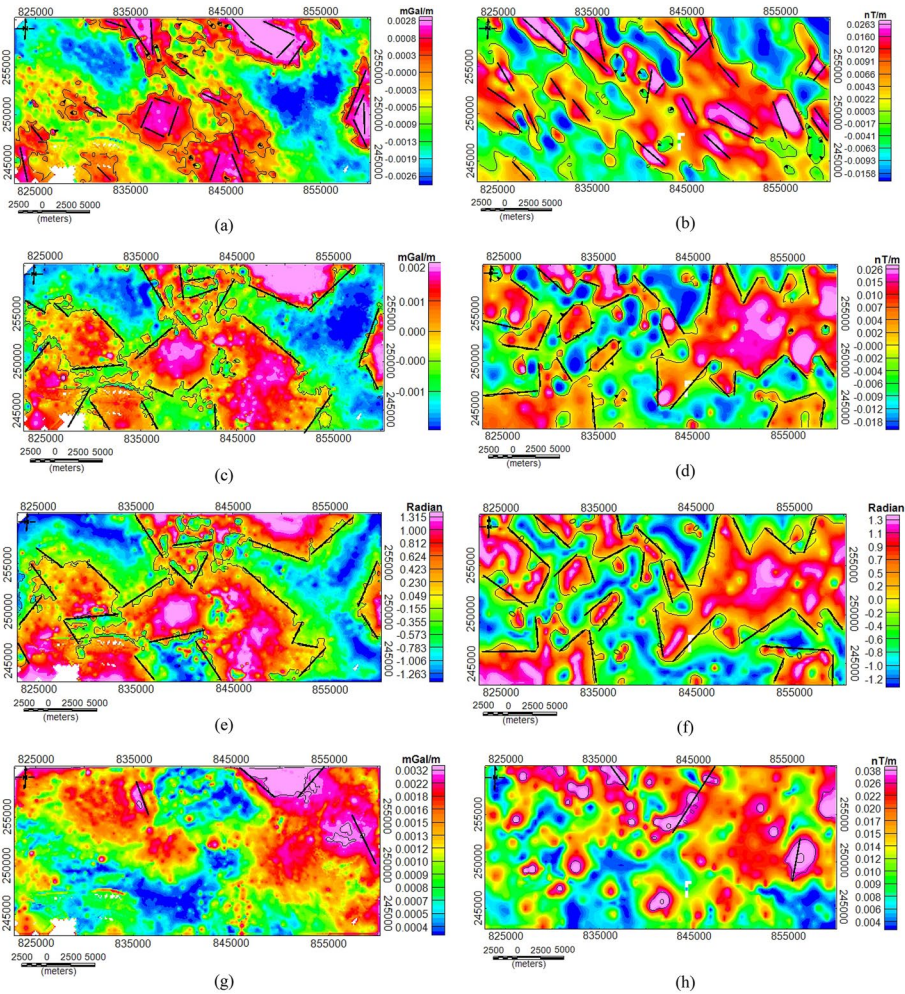


Fig. 9 **a, b** Total horizontal derivative, **c, d** first vertical derivative, **e, f** tilt angle derivative, and **g, h** analytical signal of gravity and magnetic data, respectively

areas where the gravity and magnetic fields are changing widely with depth. Consequently, the areas of zero contour separate the types of anomalies and represent the edge of the local anomalous bodies (Awad et al. 2022). The FVD map of the Bouguer anomaly (Fig. 9c) revealed faults at the west and center of the investigated area trending NE–SW and NW–SE. In the eastern and northwestern parts, a low anomaly is revealed, indicating the high thickness of the sedimentary sequences. A similar lineament trend is also indicated by the FVD map of magnetic data (Fig. 9d).

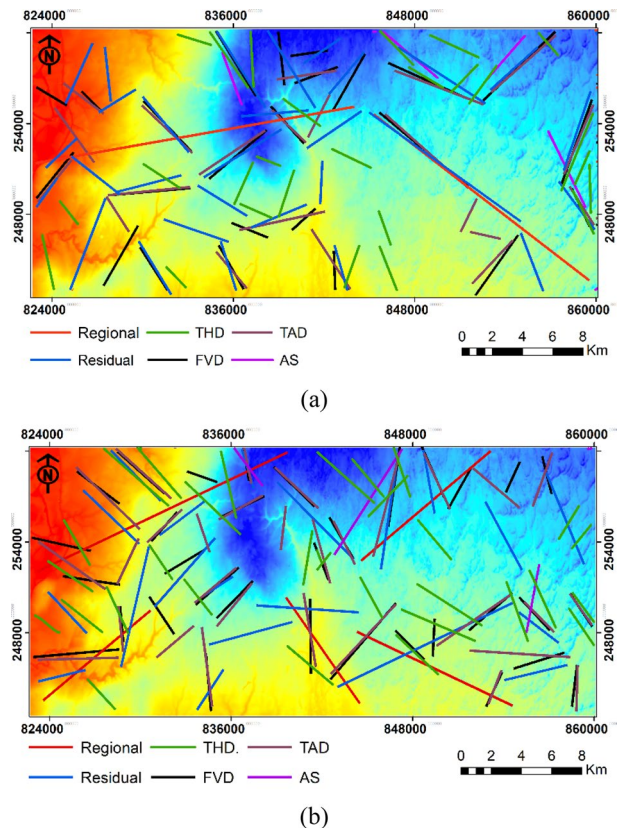
The tilt angle derivative (TAD) of the gravity and magnetic anomalies is used for delineating geological structures. TAD is applied on the Bouguer and magnetic anomaly maps, where the zero contours refer to edges of anomalous bodies, which can be related to subsurface petrophysical variations and geological features (Satyakumar et al. 2022). TAD maps of Bouguer and magnetic anomalies are illustrated in Fig. 9e and f, respectively.

TAD maps showed an almost similar trend to that of FVD, which is an indication of the dominance of vertical variation of the petrophysical properties compared to the horizontal variations.

The analytical signal (AS) of the gravity and magnetic anomalies helped in identifying the presence of gravity and magnetic sources in the maximum amplitude region. AS is used in combination with other techniques to interpret subsurface structures (Hosseini et al. 2023). The AS maps of the gravity anomaly (Fig. 9g) indicated a presence of lineament features in the northeastern and eastern parts of the area trending NE–SW and NW–SE, while the AS of the magnetic anomaly (Fig. 9h) revealed structural features in the northern and eastern part of the area.

Gravity and magnetic data are jointly interpreted to map subsurface geological structures and identify potential areas for groundwater prospecting. The lineament maps obtained from the analysis of gravity and magnetic data using potential field techniques of THD, FVD, TAD, and AS are illustrated in Fig. 10a and Fig. 10b, respectively. The delineated lineaments using various techniques for both gravity and magnetic data showed reasonable agreement. As a result, the lineaments are filtered to enhance the accuracy of the lineament identification for both gravity and magnetic. Further, the filtered maps of gravity and magnetic are integrated to form one map, which is considered a final lineaments map of the study area (Fig. 11a).

Fig. 10 Lineaments maps based on **a** gravity and **b** magnetic data obtained from different processing techniques superimposed on the digital elevation model (DEM) of the study area



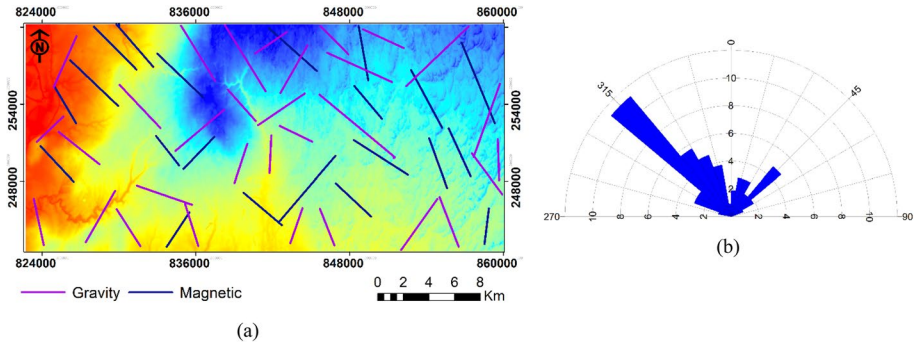
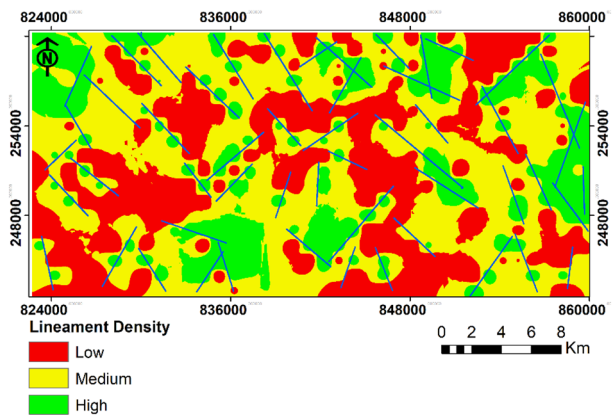


Fig. 11 **a** Final lineaments map based on the joint interpretation of gravity and magnetic data superimposed on the digital elevation model (DEM) of the study area and **b** the rose diagram shows the classification of lineaments in the study area

Fig. 12 Lineaments map of the study area based on gravity data obtained from different processing techniques



In this study, the derived lineaments map results from the manual extraction of features across multiple filtered and processed gravity and magnetic anomaly maps. Consequently, the solutions are highly subjective due to inherent biases and the inconsistency in the interpretation. However, the gravity and magnetic-based lineaments can serve as a helpful base for detailed geological investigation. The indicated lineaments of gravity and magnetic methods showed differences, especially in the eastern part of the study area, which is likely due to the differences in the petrophysical parameters that caused the anomaly. The orientation of the extracted lineament map is analyzed using a rose diagram (Fig. 11b). It indicated that the predominant orientations of the lineaments in the study area are NW–SE and NE–SW. This is the primary trend of lineaments in Hungary resulting from main stresses and strains (Bodoky et al. 2007). Accordingly, these lineaments can be classified as open and of high groundwater potential (Mohammed 2020). Based on the derived lineaments, a lineament density map is obtained (Fig. 12). It indicated that the eastern, southern, and northwestern parts of the area are associated with high lineament density, which may likely form promising zones for groundwater prospection.

4.2 Quantitative interpretation

4.2.1 Euler deconvolution (ED)

In this study, the Euler solution is applied to validate the lineaments obtained from the qualitative analysis of the potential field data and further give an approximate depth to delineated geological contacts. The Euler solutions, produced from the Bouguer and magnetic anomaly maps, are displayed in Fig. 13a and b, respectively. The structural index (SI) of zero, which is associated with geological contacts, is used to produce the ED solution with a depth accuracy of 20% and a window size of 7000 m (Njeudjang et al. 2020).

The solutions of the Bouguer anomaly (Fig. 13a) fell within the NW–SE, and NE–SW directions, in line with the lineaments obtained from potential field analysis techniques. The deepest and shallowest depths were less than 500 m and more than 1500 m, respectively. The majority of the gravity-based anomaly contacts and lineaments are located at depths between 500 and 1000 m. The ED solutions showed a close agreement with that of FVD and TAD maps. The ED solution of magnetic anomaly (Fig. 13b) showed the deepest bodies at a depth of more than 1500 m while the shallow ones at a depth of less than 500 m. The produced maps are also compatible with FVD, TAD, and AS. However, the ED solution of magnetic anomaly is less dense than that of gravity anomaly, indicating that

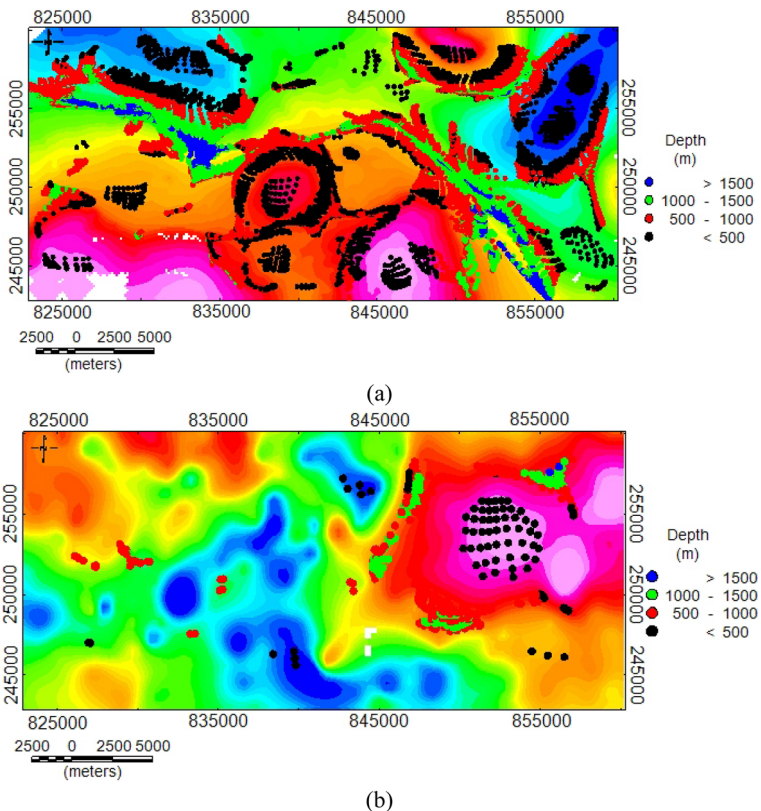


Fig. 13 Euler solutions of **a** gravity and **b** magnetic anomaly at a structural index of 0

magnetic susceptibility differences between the adjacent bodies are less compared to that of density. The eastern part of the area showed agreement between both gravity and magnetic solutions, in which this part is associated with high variations in density and magnetic susceptibility.

4.2.2 Joint interpretation of gravity and magnetic data

The joint modeling and interpretation of gravity and magnetic data constrained by lithological logs are carried out to determine the thickness of the sediments and, thus, the depth of crystalline rocks in the study area. The gravity and magnetic data are jointly and interactively inverted along three profiles (see Figs. 4 and 6). Profile 1 (A–A1) and profile 2 (B–B1) run east–west while profile 3 (C–C1) runs north–south. The initial model is assumed to consist of two layers with the depth to the basement uniformly assigned as 1.6 km based on the prior information obtained from previous geological cross-sections and reports (Tóth and Almási 2001; Haas 2012). Further, a primary density and magnetic susceptibility of 2.2 g/cm^3 and 0.001 (cgs), respectively, are assigned to the upper sedimentary layer, while 2.67 g/cm^3 and 0.002 (cgs) are assigned to the basement rocks.

Profile 1 is trending from NW to NE of the study area with a length of 37 km (Fig. 14). This profile reveals fluctuations in Bouguer and magnetic anomalies ranging from -4.5 to 4.6 mGal and 3 to 101 nT. The result of the joint inversion indicated the effect of the tectonic events, including faulting and fracturing, in forming the basement rock relief and affecting the petrophysical properties of the surrounding rocks. A series of normal and reverse faults resulted in a horst and graben topography in the metamorphic basement rocks (Tóth and Almási 2001). Accordingly, the depth of the crystalline rocks varied between 1.3 km in the north-central part of the area and 1.92 in the northwestern parts. In general, the average density and magnetic susceptibility of the sediments is 2.4 g/cm^3 and 0.0021 (cgs). For the metamorphic basement rocks, the density and magnetic susceptibility increased to 2.56 g/cm^3 and 0.0032 (cgs). The faulting process alters the surrounding rocks either by increasing or decreasing the properties of the rocks near the fault. Accordingly, The sediments and basement rocks within the graben and horst structure showed properties that are different from the surrounding rocks. For instance, the horst topography in the distance between 12.5 and 17.5 km showed a lower magnetic susceptibility of 0.0026 (cgs) and a higher density of 2.58 g/cm^3 . Those different parts are handled by separate polygons to indicate the horizontal heterogeneity within each layer.

In profile 2 (Fig. 15), the southeastern part is associated with a high magnetic anomaly of 57 nT and a low Bouguer anomaly of 1.7 mGal. The inversion resulted in a density and magnetic susceptibility of 2.34 g/cm^3 and 0.0022 (cgs) for the sedimentary sequences and 2.48 g/cm^3 and 0.0035 (cgs) for basement rocks. The broad lithological homogeneity of the basement and sedimentary fills has been disrupted by faults and fractures, both vertically and laterally (Czauner and Madl-Szonyi 2011). Accordingly, the rocks surrounding the faults showed an average density and magnetic susceptibility of 2.6 g/cm^3 and 0.0038 (cgs), respectively. The deep local basin between the normal faults in the central part of the profile in which the basement rocks showed an average density and magnetic susceptibility of 2.37 g/cm^3 and 0.003 (cgs). The depth to the basement rocks varied between 1.81 km in the southwestern part of the area and 2.2 in the southeastern parts. The deep basins exhibit good connectivity between different layers or aquifers. The presence of interconnected aquifers can facilitate the movement of water from areas of higher recharge to areas of discharge (Khazri and Gabtni 2022). Consequently, the eastern part of the study area can

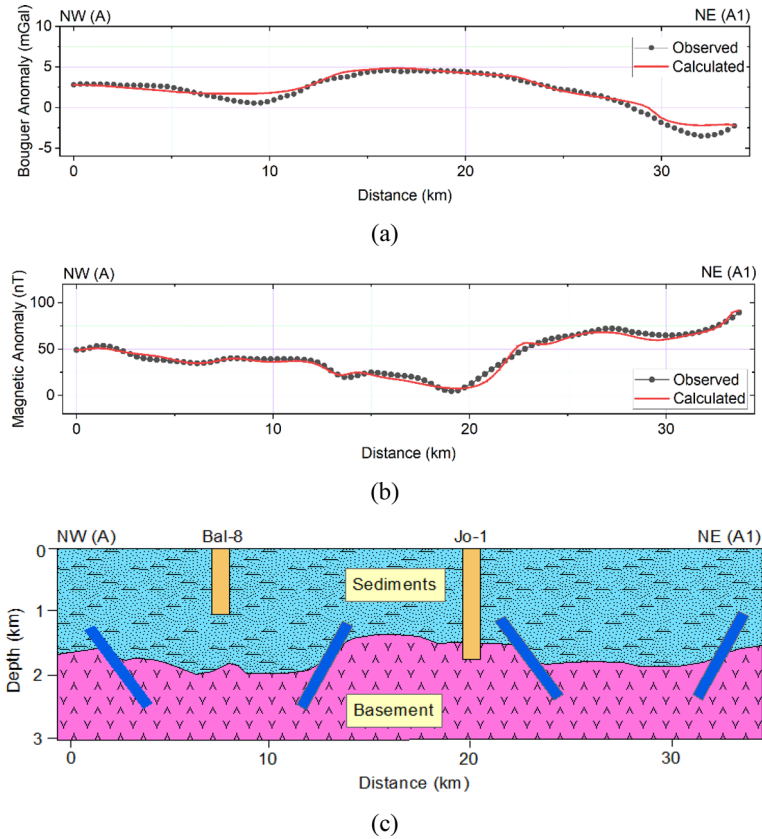


Fig. 14 Joint inversion and interpretation of the gravity and magnetic data along profile 1

be indicated as a recharge area where groundwater moves towards western and southern directions (Buday et al. 2015).

Profile 3 is running N–S with a length of 17 km (Fig. 16). This profile showed a Bouguer anomaly varied between 2.3 and 8 mGal and a magnetic anomaly ranging from 3 to 45 nT. The abrupt changes in the magnetic anomaly are explained by the presence of geological structures, while the uniformity of the Bouguer anomaly indicated the steep contact between the sedimentary and basement layers. In this profile, relatively homogeneous properties of the rocks are observed in which the sediment showed an average density and magnetic susceptibility of 2.35 g/cm^3 and 0.002 (cgs), respectively. For the basement rocks, an average density and magnetic susceptibility of 2.47 g/cm^3 and 0.0031 are observed. Reverse faults created a relatively complex geological structure that juxtaposed rocks with different physical properties. This resulted in rocks surrounding these faults having a density and magnetic susceptibility of 2.59 g/cm^3 and 0.0041 (cgs), with the depth of the basement varying from 1.25 to 1.93 km.

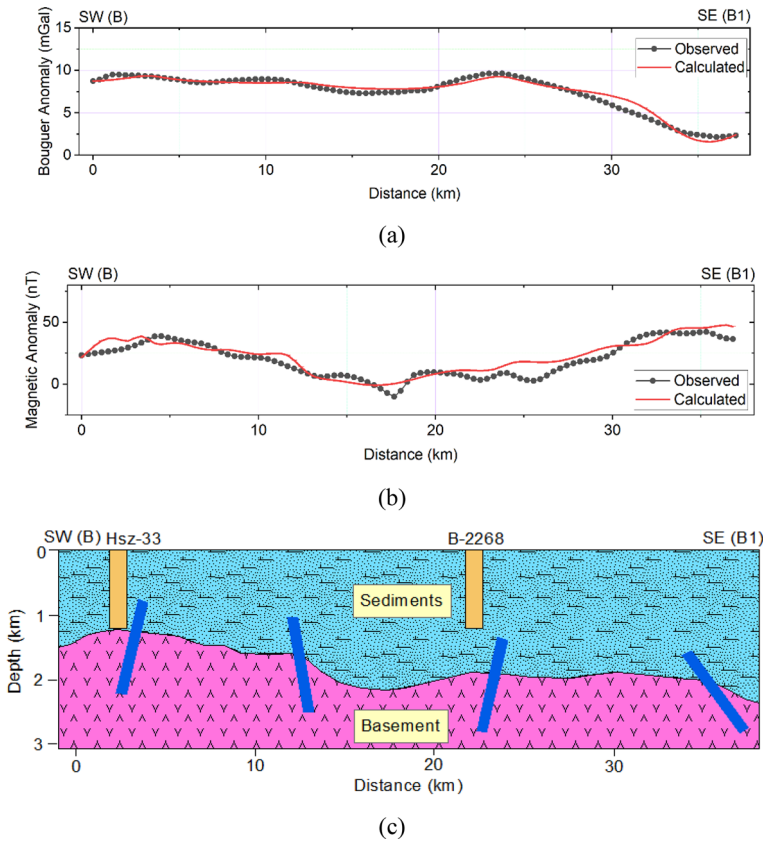


Fig. 15 Joint inversion and interpretation of the gravity and magnetic data along profile 2

4.3 Hydrostratigraphical investigation

Based on the lithological description of the existing boreholes, the main four hydrostratigraphic units, including Nagyalföld, Algyó, Endrőd, Badenian, and Pre-Neogene basement, were indicated. The geometry of the hydrostratigraphical units is illustrated in Table 1. Nagyalföld aquifer covers the surface of the Debrecen area with a thickness range between 600 and 1073 m. The maximum thickness is in Bal-2 borehole in the northwestern part, while the minimum is in B-2268 borehole in the southern part of the study area. The Nagyalföld aquifer unit consists of sand, gravel, silt, and clay, which have been deposited by rivers and streams (Gyalog and Síkhegyi 2005). The permeability of the Nagyalföld aquifer ranges from 100 to 1000 mD, and the variation is based on the shale content present in the aquifer materials (Tóth and Almási 2001). The Algyó and Endrőd units act as barriers to groundwater flow and are composed of siltstone and marls, respectively. The average permeability of these units is approximated to 0.1 mD, making it a main aquitard in the study area. The Algyó and Endrőd units are regionally extensive aquitard with an average thickness of 400 m; however, it shows a discontinuity in some localities, making Nagyalföld aquifer in direct contact with the underlying Miocene aquifer. The Miocene aquifer is

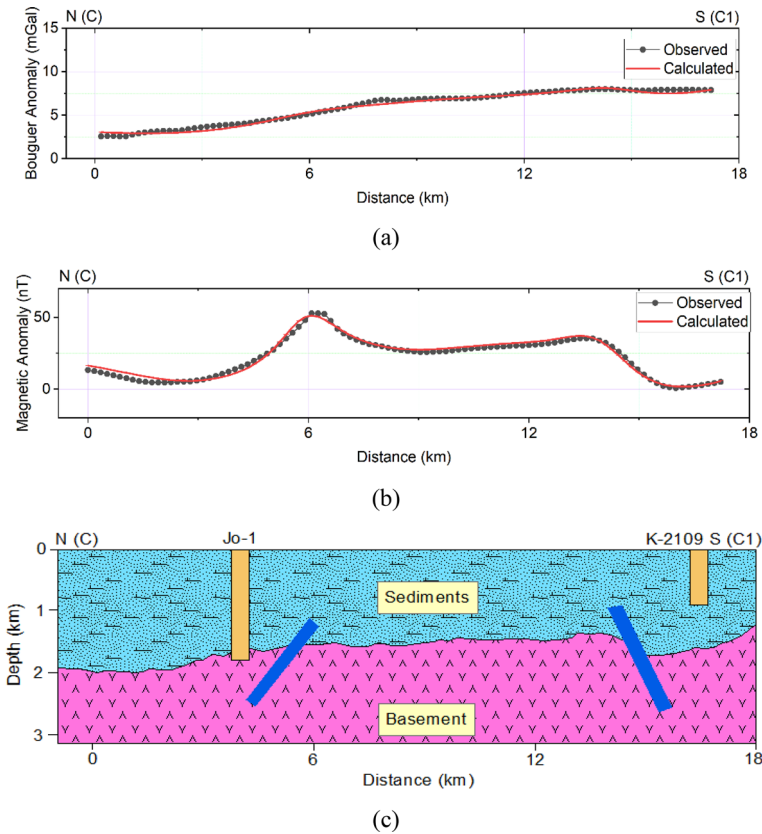


Fig. 16 Joint inversion and interpretation of the gravity and magnetic data along profile 3

a significant hydrostratigraphic unit comprised of various sedimentary rocks, including sandstones, silt, and clays. The permeable sandstone layers within this formation of 100 mD permeability serve as a good reservoir for the thermal water (Buday et al. 2015). The thickness of the Miocene formation varies between 60 m in the northwestern part and more than 557 m in the northern part of the study area. These formations rest over the crystalline Pre-Neogene basement rocks of almost zero permeability. However, the permeability increases due to fracturing and faulting (Tóth and Almási 2001).

The joint interpretation of gravity and magnetic data supported by lithological logs effectively delineated the geological structures and basement rock relief. However, a detailed geological and hydro-geophysical survey is recommended for more precise detection and characterization of the geological units. For instance, the integration of gravity and magnetic with electrical methods can more accurately indicate the lithology distribution. Moreover, geophysical well logging allows for the investigation of hydrogeological and petrophysical parameters, which can be useful for predicting the productivity of groundwater aquifers.

Table 1 The geometry of the main hydrostratigraphical units obtained from the description of the lithological logs in the study area

Well name	Elevation	Nagyalföld		Algyó		Endrőd		Bedenian		Pre-Neogene	
		From	To	From	To	From	To	From	To	From	To
Bal-2	93	93	-979.9	-979.9	-1131.9	-	-	-	-	-	-
Bal-4	94	94	-831.4	-831.4	-937	-937	-1061.9	-1061.9	-1120.4	-	-
Bal-7	113	113	-767.8	-767.8	-965.8	-	-	-965.8	-	-	-
Bal-8	113	113	-887.8	-887.8	-1007	-	-	-	-	-	-
B-2268	122	122	-538	-538	-978	-	-	-	-	-	-
K-2109	111	111	-543	-543	-651	-651	-912	-	-	-	-
Hb-3	148	148	-619.8	-619.8	-815.8	-	-	-815.8	-	-	-
Hsz-11	97	97	-954.2	-954.2	-1210.2	-1210.2	-	-	-	-	-
Hsz-33	105	105	-958	-958	-1193.1	-1193.1	-1233	-1233	-	-	-
Jo-1	149	149	-557	-557	-853	-853	-1095	-1095	-1652	-1652	-1798

5 Conclusion

The overall objective of this research was to use potential field geophysical methods to support groundwater prospecting in the Debrecen area, Eastern Hungary. Gravity and magnetic data are jointly interpreted and modeled using potential field techniques and geophysical inversion to delineate the subsurface lithology and geological structures. The outcomes can be summarized as follows:

- The potential field data is subjected to spectral analysis that provided a robust separation of the shallow and deep anomalies that corresponded to the sedimentary and crystalline rocks, respectively. The discrepancy is attributable to the distinctive petrophysical characteristics that influence the measurements.
- Potential field techniques, including THD, FVD, TAD, and AS, are integrated to provide a detailed lineament map of the study area. This integration enabled the identification and mapping of geological structures that are mostly found in NW–SE and NE–SW trends. As a result, a lineament density map is constructed and indicates that the eastern, southern, and northwestern parts of the study area are associated with higher structure density. Moreover, Euler deconvolution is applied to confirm the results of the potential field techniques and predict the depths of the delineated lineaments.
- The thickness of the sedimentary sequences and the depth to the bottom of the Pre-Neogene basement rocks are delineated with joint inversion of gravity and magnetic data. The results indicated that the depth to the basement varies between 1.18 km in the southwestern part and 2.2 km in the southeast. Moreover, the geometry of the different hydrostratigraphic units, including the Nagyalföld, Algyő, Endrőd, and Badenian units, is detected using the lithological logs from the drilled boreholes.
- Overall, the results of this study highlight the effectiveness of the joint interpretation of gravity and magnetic data to support groundwater prospecting efforts. However, a detailed geophysical investigation is recommended; for instance, direct current electrical resistivity and well-logging methods allow for accurate delineation of aquifer geometry and estimation of the hydraulic properties of the aquifers.

Acknowledgements The research was funded by the Sustainable Development and Technologies National Program of the Hungarian Academy of Sciences (FFT NP FTA). The research was partly carried out in the Project No. K-135323 supported by the National Research, Development and Innovation Office (NKFIH), Hungary. The second author thanks the support of NKFIH. The authors would like to thank the Supervisory Authority for Regulatory Affairs (SARA) for providing the necessary data to carry out this research.

Funding Open access funding provided by University of Miskolc. The research was funded by the Sustainable Development and Technologies National Program of the Hungarian Academy of Sciences (FFT NP FTA).

Data availability The data is available by the corresponding author upon request.

Declarations

Conflict of interest Norbert P. Szabó is an editor of this journal and recused himself from all decisions about this paper. Otherwise, the authors have no competing interests to declare that are relevant to the content of this article.

Open Access This article is licensed under a Creative Commons Attribution 4.0 International License, which permits use, sharing, adaptation, distribution and reproduction in any medium or format, as long as you give appropriate credit to the original author(s) and the source, provide a link to the Creative Commons licence, and indicate if changes were made. The images or other third party material in this article are included in the article's Creative Commons licence, unless indicated otherwise in a credit line to the material. If material is not included in the article's Creative Commons licence and your intended use is not permitted by statutory regulation or exceeds the permitted use, you will need to obtain permission directly from the copyright holder. To view a copy of this licence, visit <http://creativecommons.org/licenses/by/4.0/>.

References

- Abdelrady M, Moneim MA, Alarifi SS et al (2023) Geophysical investigations for the identification of subsurface features influencing mineralization zones. *J King Saud Univ Sci* 35:102809. <https://doi.org/10.1016/j.jksus.2023.102809>
- Alvandi A, Deniz Toktay H, Nasri S (2022) Application of direct source parameter imaging (direct local wave number) technique to the 2D gravity anomalies for depth determination of some geological structures. *Acta Geophys* 70:659–667. <https://doi.org/10.1007/s11600-022-00750-6>
- Awad MS, El Kadi HH, Abbas AM, Awad Sultan Araffa S (2022) Delineation of subsurface structures using gravity interpretation around Nabaa Al Hammara area, Wadi El Natrun Egypt. *NRIAG J Astron Geophys* 11:282–292. <https://doi.org/10.1080/20909977.2022.2085992>
- Baranov V, Naudy H (1964) Numerical calculation of the formula of reduction to the magnetic pole. *Geophysics* 29:67–79
- Basantaray AK, Mandal A (2022) Interpretation of gravity–magnetic anomalies to delineate subsurface configuration beneath east geothermal province along the Mahanadi rift basin: a case study of non-volcanic hot springs. *Geotherm Energy* 10:1–27. <https://doi.org/10.1186/s40517-022-00216-4>
- Bendefy L (1968) Debrecen városi belső süllyedésének hidrogeológiai vonatkozásai (hydrogeologic aspects of settlement subsidences observed in Debrecen). *Hidrológiai Közlöny* 48:549–559
- Blakely RJ (1996) Potential theory in gravity and magnetic applications. Cambridge University Press
- Bodoky T, Balla Z (2015) Gravity lineament map of Hungary final report M gravity lineamen map of fungus Topic leader : B Odoky T the other Contributed by : p GRILL E RN
- Bodoky TJ, Balla Z, Gulyás Á, et al (2007) Gravity lineament map of Hungary. OTKA Kutatási Jelentések OTKA Research Reports
- Buday T, Szűcs P, Kozák M et al (2015) Sustainability aspects of thermal water production in the region of Hajdúszoboszló-Debrecen, Hungary. *Environ Earth Sci* 74:7511–7521. <https://doi.org/10.1007/s12665-014-3983-1>
- Buday T, Püspöki Z (2011) B05 Facies variations detected by well log correlation in a geothermal reservoir (Újfalu Formation) around Debrecen, Hungary. In: 6th congress of balkan geophysical society
- Chen Q, Dong Y, Tan X et al (2022) Application of extended tilt angle and its 3D Euler deconvolution to gravity data from the Longmenshan thrust belt and adjacent areas. *J Appl Geophys* 206:104769. <https://doi.org/10.1016/j.jappgeo.2022.104769>
- Czauner B, Madl-Szonyi J (2011) The function of faults in hydraulic hydrocarbon entrapment: theoretical considerations and a field study from the trans-tisza region, Hungary. *AAPG Bull* 95:795–811
- Darwish SM, Saibi H, Gabr A, Mohamed MM (2021) Microgravity monitoring of groundwater dynamics in a shallow aquifer in Al-Ain (Abu Dhabi Emirate, United Arab Emirates): an opportunity for understanding aquifer hydrodynamics in arid regions. *Environ Earth Sci* 80:1–17
- Díalos S, Alexopoulos JD, Vassilakis E, Poulos SE (2022) Investigation of the structural control of a deltaic valley with geophysical methods. The case study of Pineios river delta (Thessaly, Greece). *J Appl Geophys* 202:104652. <https://doi.org/10.1016/j.jappgeo.2022.104652>
- Ekinci YL, Yiğitbaş E (2015) Interpretation of gravity anomalies to delineate some structural features of Biga and Gelibolu peninsulas, and their surroundings (north-west Turkey). *Geodin Acta* 27:300–319. <https://doi.org/10.1080/09853111.2015.1046354>
- Elawadi E, Mogren S, Ibrahim E et al (2012) Utilizing potential field data to support delineation of groundwater aquifers in the southern Red Sea coast, Saudi Arabia. *J Geophys Eng* 9:327–335. <https://doi.org/10.1088/1742-2132/9/3/327>
- Eldosouky AM, Pham LT, Mohmed H, Pradhan B (2020) A comparative study of THG, AS, TA, Theta, TDX and LTHG techniques for improving source boundaries detection of magnetic data using synthetic models: a case study from G. Um Monqul, North Eastern Desert Egypt. *J Afr Earth Sci* 170:103940. <https://doi.org/10.1016/j.jafrearsci.2020.103940>

- Erdélyi M (1976) Outlines of the hydrodynamics and hydrochemistry of the Pannonian Basin. *Acta Geol Hung* 20:287–309
- Essa KS, Abo-Ezz ER, Géraud Y (2021) Utilizing the analytical signal method in prospecting gravity anomaly profiles. *Environ Earth Sci* 80:1–21
- Featherstone WE, Dentith MC (1997) A geodetic approach to gravity data reduction for geophysics. *Comput Geosci* 23:1063–1070
- Fejes Z, Szűcs P, Turai E et al (2021) Regional hydrogeology of the tokaj mountains world heritage site, north-east Hungary. *Acta Montanistica Slovaca* 26:18–34
- Fülöp J (1989) Bevezetés Magyarország geológiájába. Akadémiai Kiadó, Cambridge
- Ghosh GK (2022) Delineation of major subsurface structural features and source depth locations using 3-D Euler deconvolution of gravity data at north-eastern part of India. *Acta Geophys* 70:2033–2044. <https://doi.org/10.1007/s11600-022-00829-0>
- Gyalog L, Síkhegyi F (2005) Geological Map of Hungary, 1: 100,000. Geological Institute of Hungary, Budapest (In Hungarian) Digital version Retrieved December 1:2008
- Haas J (2012) Geology of Hungary. Springer, Cham
- Horváth F (1993) Towards a dynamic model for the formation of the Pannonian basin. *Tectonophysics* 226:333–357
- Hosseini SA, Keshavarz Farajkhah N, Kianoush P et al (2023) Determination of the boundaries of anomaly potential field with analytical signal filter and its orthogonal derivative in Qeshm Island SE Iran. *SSRN Electron J* 14:100053. <https://doi.org/10.2139/ssrn.4332255>
- Juhász G (1991) Lithostratigraphical and sedimentological framework of the Pannonian (sl) sedimentary sequence in the Hungarian Plain (Alföld), Eastern Hungary. *Acta Geol Hung* 34:53–72
- Kearey P, Brooks M, Hill I (2002) An introduction to geophysical exploration. Wiley, Hoboken
- Keating P (1995) A simple technique to identify magnetic anomalies due to kimberlite pipes. *Explor Min Geol* 4:121–125
- Kenyo B, Koumetio F, Kwekam M, Kengni L (2023) Characteristics of lineaments using gravity data in the Eastern Cameroon: structural, hydrogeological and natural risks implications. *J Afr Earth Sc* 202:104886. <https://doi.org/10.1016/j.jafrearsci.2023.104886>
- Khazri D, Gabtni H (2022) New structural model to understanding the subsurface hydrogeology system of the Ouled Asker groundwater, Central Tunisian Atlasic foreland, derived from an integrated geophysical approach. *Arabian J Geosci* 15. <https://doi.org/10.1007/s12517-022-09966-8>
- Kiss J (2006) Bouguer anomaly map of Hungary. *Geophys Trans* 45:99–104
- Kiss J (2018) Gravitational, magnetic and aerial geophysical databases. *Hung Geophys* 59:129–148
- Kiss T, Hernesz P, Sümeghy B et al (2015) The evolution of the Great Hungarian Plain fluvial system—fluvial processes in a subsiding area from the beginning of the Weichselian. *Quatern Int* 388:142–155. <https://doi.org/10.1016/j.quaint.2014.05.050>
- Kovács P, Körmendi A (1999) Geomagnetic repeat station survey in Hungary during 1994–1995 and the secular variation of the field between 1950 and 1995. *Geophys Trans* 42:107–132
- Kozák M, McIntosh RW, Buday T (2010) Geotermikus rendszerek fenntarthatóságának integrált modellezése. Hidrogeotermikus rendszerek és földtani vetületeik. Debreceni Egyetem, Debrecen
- Kronome B, Baráth I, Nagy A et al (2014) Geological model of the Danube Basin; transboundary correlation of geological and geophysical data. *Slovak Geol Mag* 14:17–35
- Liebe P (2006) Groundwaters in Hungary. Ministry for environment and water, Budapest
- Mádl-Szőnyi J, Tóth J (2009) A hydrogeological type section for the Duna-Tisza Interfluve, Hungary. *Hydrogeol J* 17:961–980. <https://doi.org/10.1007/s10040-008-0421-z>
- Mádl-Szőnyi J, Czauner B, Iván V et al (2019) Confined carbonates—regional scale hydraulic interaction or isolation? *Mar Pet Geol* 107:591–612. <https://doi.org/10.1016/j.marpetgeo.2017.06.006>
- Marquardt DW (1963) An algorithm for least-squares estimation of nonlinear parameters. *J Soc Ind Appl Math* 11:431–441
- Melouah O, Pham LT (2021) An improved ILTHG method for edge enhancement of geological structures: application to gravity data from the Oued Righ valley. *J Afr Earth Sci* 177:104162. <https://doi.org/10.1016/j.jafrearsci.2021.104162>
- Miller HG, Singh V (1994) Potential field tilt—a new concept for location of potential field sources. *J Appl Geophys* 32:213–217
- Mohamed A, Abdelrady M, Alshehri F et al (2022a) Detection of mineralization zones using aeromagnetic data. *Appl Sci* 12(18):9078. <https://doi.org/10.3390/app12189078>
- Mohamed A, Al Deep M, Abdelrahman K, Abdelrady A (2022b) Geometry of the magma chamber and curie point depth beneath Hawaii Island: inferences from magnetic and gravity data. *Front Earth Sci* 10:1–17. <https://doi.org/10.3389/feart.2022.847984>

- Mohammed MAA, Szabó NP, Szűcs P (2023a) Assessment of the Nubian aquifer characteristics by combining geoelectrical and pumping test methods in the Omdurman area, Sudan. *Model Earth Syst Environ* 9:4363–4383. <https://doi.org/10.1007/s40808-023-01767-6>
- Mohammed MAA, Szabó NP, Szűcs P (2023b) Characterization of groundwater aquifers using hydrogeophysical and hydrogeochemical methods in the eastern Nile River area, Khartoum State Sudan. *Environ Earth Sci* 82(9):1–21. <https://doi.org/10.1007/s12665-023-10915-1>
- Mosbahi H, Jrad A, Dhaoui M et al (2023) Constrained 3D gravity modelling of a multilayered aquifer system in an arid region: Case of Sebkhath El Bhira basin (Central Tunisia). *J Appl Geophys* 210:104950. <https://doi.org/10.1016/j.jappgeo.2023.104950>
- Murty BVS, Raghavan VK (2002) The gravity method in groundwater exploration in crystalline rocks: a study in the peninsular granitic region of Hyderabad, India. *Hydrogeol J* 10:307–321. <https://doi.org/10.1007/s10040-001-0184-2>
- Mohammed MAA (2020) The use of Landsat ETM+ in hydrogeological investigation in basement terrain, Hamissana area, N–E Sudan. *Humanit Nat Sci J*. <https://doi.org/10.53796/HNSJ1625>
- Nishijima J, Naritomi K (2017) Interpretation of gravity data to delineate underground structure in the Beppu geothermal field, central Kyushu, Japan. *J Hydrol: Reg Stud* 11:84–95. <https://doi.org/10.1016/j.ejrh.2015.11.022>
- Njeudjang K, Abate Essi JM, Kana JD et al (2020) Gravity investigation of the Cameroon volcanic line in Adamawa region: geothermal features and structural control. *J Afr Earth Sc* 165:103809. <https://doi.org/10.1016/j.jafrearsci.2020.103809>
- Nowell DAG (1999) Gravity terrain corrections—an overview. *J Appl Geophys* 42:117–134
- Núñez-Demarco P, Bonilla A, Sánchez-Bettucci L, Prezzi C (2023) Potential-field filters for gravity and magnetic interpretation: a review. Springer, Netherlands
- Pawłowski RS (1994) Green's equivalent-layer concept in gravity band-pass filter design. *Geophysics* 59:69–76
- Reynolds JM (2011) An introduction to applied and environmental geophysics. Wiley, Hoboken
- Rubin Y, Hubbard SS (2006) *Hydrogeophysics*. Springer, Cham
- Satyakumar AV, Pandey AK, Singh AP, Tiwari VM (2022) Delineation of structural and tectonic features in the Mahanadi basin, eastern India: New insights from remote sensing and land gravity data. *J Asian Earth Sci* 227:105116. <https://doi.org/10.1016/j.jseaes.2022.105116>
- Sharma B, Geldart LP (1968) Analysis of gravity anomalies of two-dimensional faults using fourier transforms. *Geophys Prospect* 16:77–93
- Simon S, Mádl-Szőnyi J, Müller I, Pogácsás G (2011) Conceptual model for surface salinization in an overpressured and a superimposed gravity-flow field, Lake Kelemtenszék area, Hungary. *Hydrogeol J* 19:701–717. <https://doi.org/10.1007/s10040-011-0711-8>
- Spector A, Grant FS (1970) Statistical models for interpreting aeromagnetic data. *Geophysics* 35:293–302
- Szabó NP, Kiss A, Halmágyi A (2015a) Hydrogeophysical characterization of groundwater formations based on well logs: case study on cenozoic clastic aquifers in East Hungary. *Geosci Eng* 4:45–71
- Szabó NP, Kormos K, Dobróka M (2015b) Evaluation of hydraulic conductivity in shallow groundwater formations: a comparative study of the Csókás' and Kozeny-Carman model. *Acta Geod Geoph* 50:461–477. <https://doi.org/10.1007/s40328-015-0105-9>
- Székely F, Deák J, Szűcs P et al (2020) Verification of radiocarbon transport predicted by numerical modeling in the porous formation of NE Hungary considering paleo-hydrogeology. *Radiocarbon* 62:219–233. <https://doi.org/10.1017/RDC.2019.84>
- Szűcs P, Szabó NP, Zubair M, Szalai S (2021) Innovative hydrogeophysical approaches as aids to assess hungarian groundwater bodies. *Appl Sci* 11:2099. <https://doi.org/10.3390/app11052099>
- Talwani M (1964) Computation of magnetic anomalies caused by two dimensional structures of arbitrary shape. *Comput Miner Ind* 1:464–480
- Talwani M, Worzel JL, Landisman M (1959) Rapid gravity computations for two-dimensional bodies with application to the Mendocino submarine fracture zone. *J Geophys Res* 64:49–59
- Thompson DT (1982) EULDPH: a new technique for making computer-assisted depth estimates from magnetic data. *Geophysics* 47:31–37
- Timár G, Sümegi P, Horváth F (2005) Late quaternary dynamics of the Tisza River: evidence of climatic and tectonic controls. *Tectonophysics* 410:97–110. <https://doi.org/10.1016/j.tecto.2005.06.010>
- Tóth J, Almási I (2001) Interpretation of observed fluid potential patterns in a deep sedimentary basin under tectonic compression: hungarian great plain, pannonian basin. *Geofluids* 1:11–36. <https://doi.org/10.1046/j.1468-8123.2001.11004.x>
- Vajk R (1956) Bouguer corrections with varying surface density. *Geophysics* 21:1004–1020
- Verduzco B, Fairhead JD, Green CM, MacKenzie C (2004) New insights into magnetic derivatives for structural mapping. *Lead Edge* 23:116–119
- Webring M (1985) SAKI: A Fortran program for generalized linear inversion of gravity and magnetic profiles

- Won JJ, Bevis M (1987) Computing the gravitational and magnetic anomalies due to a polygon: algorithms and Fortran subroutines. *Geophysics* 52:232–238. <https://doi.org/10.1190/1.1442298>
- Zareie V, Moghadam RH (2019) The Application of theta method to potential field gradient tensor data for edge detection of complex geological structures. *Pure Appl Geophys* 176:4983–5001. <https://doi.org/10.1007/s00024-019-02226-z>